Natural Products and Bioprospecting

Compounds from *Agathis dammara* exert hypoglycaemic activity by enhancing glucose uptake: lignans, terpenes and others

Zhe-Wei Yu[1,2†], Bang-Ping Cai[3†], Su-Zhi Xie[4], Yi Zhang[1], Wen-Hui Wang[1], Shun-Zhi Liu[1], Yan-Lin Bin[1], Qi Chen[1], Mei-Juan Fang[1], Rong Qi[2], Ming-Yu Li[1*] and Ying-Kun Qiu[1*]

Abstract

In this study, two new kaurane diterpenes (1**6**, **17**), together with 12 lignans (**1–12**), a triterpene (**15**), and two other compounds (**13**, **14**) were isolated from the woods of *Agathis dammara*. The structure of the new compound was determined by HR ESIMS and 1D/2D NMR spectroscopy, and its absolute configuration was determined by electronic circular dichroism (ECD) exciton chirality method. Compounds **5**, **11**, **14** exhibit significant hypoglycaemic activity in zebrafish, and their mechanism of action is to enhance glucose uptake in zebrafish.

Keywords *Agathis dammara*, Lignans, Terpenes, Hypoglycaemic, Glucose uptake

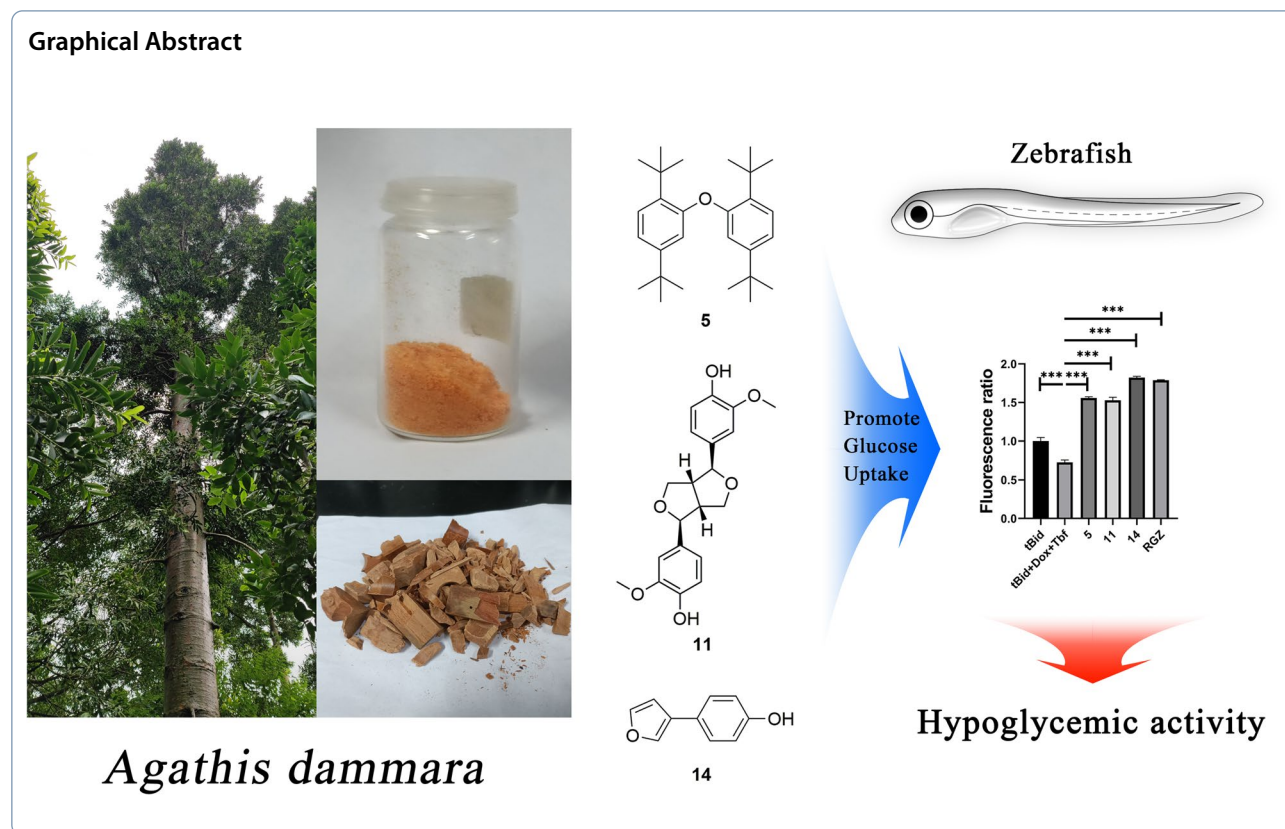†Zhe-Wei Yu and Bang-Ping Cai contributed equally.

*Correspondence:
Ming-Yu Li
limingyu@xmu.edu.cn
Ying-Kun Qiu
qyk@xmu.edu.cn
Full list of author information is available at the end of the article

Graphical Abstract

Agathis dammara

1 Introduction

Agathis dammara (Lamb.) Rich is a kind of arbor in the family Araucariaceae and the genus *Agathis* [1]. The origin of *A. dammara* is Malaysia and the Philippines, and it has been introduced to Xiamen, Quanzhou, Fuzhou and other places in China [1]. The trunk of *A. dammara* is rich in resin, which is widely used in industry and medicine [2]. Malaysians use this resin to treat a variety of complex and inflammation-related ailments including arthritis, headaches, muscle pain, burns, fever, diarrhoea, abdominal pain [3]. Related studies have shown that *A. dammara* has potential activities of hypoglycaemic, hypolipidemic, antioxidant, anti-inflammatory [2]. In our parallel study, we found that the total diterpene component of *A. dammara* and its rich monomeric compound, araucarone could effectively mitigate the inflammatory response in vascular smooth muscle cells, and consequently impede the progression of abdominal aortic aneurysm through suppressing NF-kappaB/NLRP3 pathway activation [4]. In the current study, two new kaurane diterpenes (1**6**, **17**), together with 12 lignans (**1–12**), a triterpene (**15**), and two other compounds (**13**, **14**) were isolated from the woods of *A. dammara* (Fig. 1). Presented herein are the isolation, structure identification, hypoglycaemic

biological evaluation and biological mechanism studies of these compounds.

2 Results and discussion

2.1 Structural identification of new compounds

(3β)-3,13-Dihydroxykaur-16-en-2-one (**16**) is white powder. HRESIMS shows that the molecular formula is $C_{20}H_{30}O_3$ (*m/z* 319.2265 [M+H]$^+$, calcd 319.2268), and the degree of unsaturation is 6. UV spectra indicated carbon–carbon double bond ($\lambda_{max} = 210$ nm), IR spectra indicated carbonyl ($\sigma_{min} = 1712$ cm^{-1}) and hydroxyl ($\sigma_{min} = 3424$ cm^{-1}). There were 3 methyl signals in ^{1}H-NMR of **16** at δ_H 0.70 (br s, 3H, H-18), 1.19 (s, 3H, H-19), and 0.97 (s, 3H, H-20). In addition, two alkene hydrogen signals at δ_H 4.85 (m, H-17), 5.00 (m, H-17), and one methine bearing to hydroxyl at δ_H 3.87 (br s, H-3) were found. In the ^{13}C-NMR of **16**, the signal at δ_C 210.7 (C-2) suggested the presence of carbonyl. The DEPT spectrum showed 3 primary carbons, 8 secondary carbons, 3 tertiary carbons, and 6 quaternary carbons, including a quaternary carbon connected to a hydroxyl at δ_C 80.0 (C-13). The methyl remote coupling signal of HMBC can confirm that the δ_H 0.70 (br s, CH$_3$-18), 1.19 (s, CH$_3$-19) connecting to δ_C 45.3 (C-4) then to 82.8 (C-3) and 54.4 (C-5), and δ_H 0.97 (s, CH$_3$-20) connecting to δ_C 45.2 (C-10) then to

Yu *et al. Natural Products and Bioprospecting*　　(2024) 14:23

Page 3 of 9
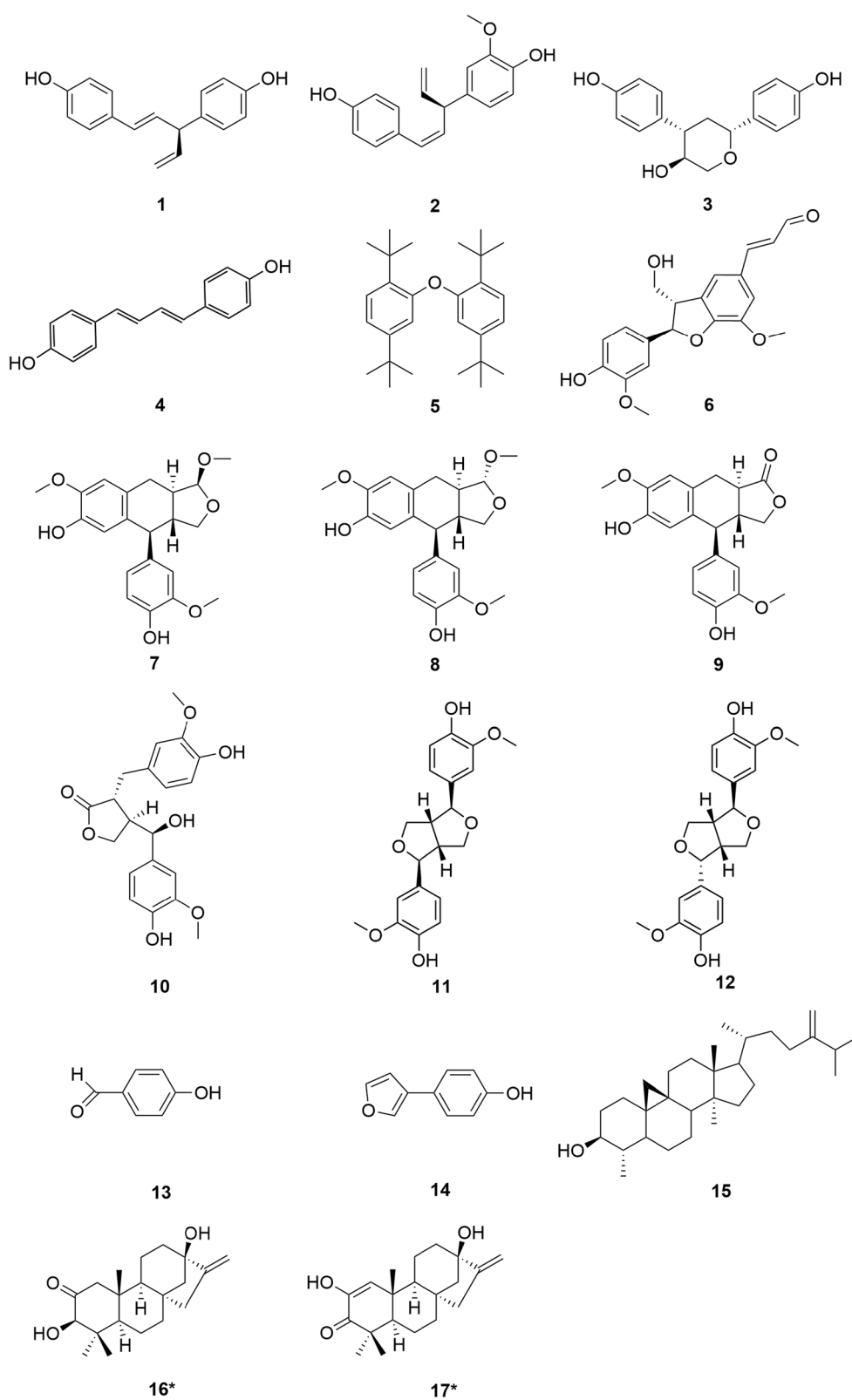
Fig. 1 Structure of isolated compounds from the woods of *Agathis dammara* (*new compounds)

Yu *et al. Natural Products and Bioprospecting*   (2024) 14:23

Page 4 of 9

53.2 (C-1), 54.4 (C-5) and 54.0 (C-9). The coupling from δ_H 3.87 (br s, H-3), 2.03; 2.64 (m; dd, H-1) and δ_C 210.7 (C-2) confirmed the position of carbonyl at C-2. In the HMBC spectrum, correlations could be observed from δ_H 4.85; 5.00 (m; m, H-17) at the end side of the alkene to δ_C 155.3 (C-16), and then to the quaternary carbon 80.0 (C-13) and methylene 47.1 (C-15). Moreover, the HMBC

correlations showed that there is an extra D ring in the closure of C-8, 13, 14, 15, and 16, which proves that this is a tetracyclic diterpene (Fig. 2A). **16** is very similar to the structure of the known compound excoecarin K [5]. Excoecarin K is an enantio-kaurane tetracyclic diterpene, indicating that **16** should also be a tetracyclic diterpene of the kaurane skeleton. The difference between **16** and

Fig. 2 Structural elucidation of compounds **16**, **17**. **A** COSY and key HMBC signals. **B** NOESY correlations and relative configurations. **C** ECD spectral of **16**, **17** versus calculated values
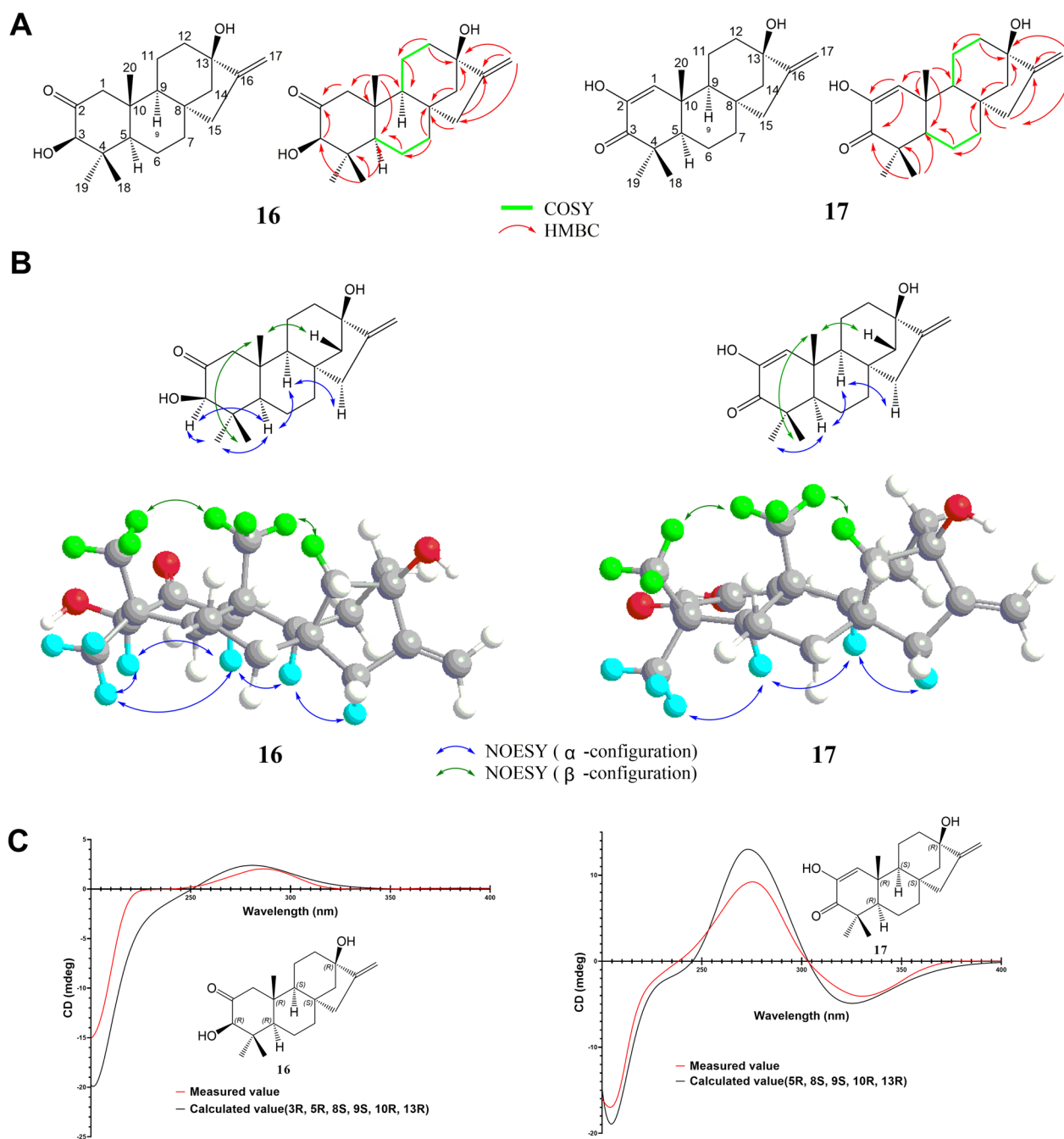
excoecarin K is that C-13 of **16** has a higher chemical shift (δ_C 43.7 to 80.0) because 13-H is replaced by 13-OH. In NOESY, there are related signals of δ_H 0.97 (s, CH_3-20), 0.70 (br s, CH_3-18), and 2.04 (m, H-14β), which can indicate that C-14 on the C ring is tilted in the same direction as CH_3-20, CH_3-18; δ_H 1.19 (s, CH_3-19), there are also correlation signals between 1.49 (m, H-5), 1.29 (br s, H-9), 3.87 (br s, H-3), and 2.12 (br d, H-15α), indicating that the D ring is tilted in the direction opposite to that of C-14, that is, the configurations of C-15, C-16 and CH_3-19, H-5 and H-9 are consistent, that is, CH_3-20, CH_3-17, CH_3-18, 3-OH, 13-OH are β configurations, H-5, H-9, C-15, and C-16 are in α configuration (Fig. 2B). The data determined by ECD showed that the absolute configuration of the compound is 3*R*, 5*R*, 8*S*, 9*S*, 10*R*, and 13*R* (Fig. 2C).

By comparison the ^{13}C-NMR signals of **17** and **16**, the difference between them leis in A ring. The C-3 position changed from a hydroxyl connected methine to a carbonyl, which shifted from δ_C 82.8 to δ_C 201.0. In addition, the -CH_2CH(OH)- moiety at C-1, 2 position of **16** with signals at δ_C 53.2, 210.7 changes to a hydroxyl connected alkene double bone (δ_C 128.4 and 144.3) to form an α,β-unsaturated ketone structure. on the aids of HSQC, COSY and HMBC, the planar structure could be established as shown in Fig. 2A. The comparison of NOE correlations (Fig. 2B), optical rotation, ECD spectrum and calculated value showed that the absolute configuration of **17** is consistent with **16** (Fig. 2C).

Other isolated compounds were identified from their NMR and MS data, as well as by comparing these data with reported values, and they were: hinokiresinol (**1**) [6], methoxynyasol (**2**) [7], sugiresinol (**3**) [8], bis (4-hydroxyphenyl) buta-1,3-diene (**4**) [9], 2,2'-oxybis(1,4)-ditertbutylbenzene (**5**) [10], balanophonin (**6**) [11], todolactol C (**7**) [12], (1*R*,3a*R*,4*S*,9a*R*)-1,7-dimethoxy-4-(4'-hydroxy-3'-methoxyphenyl)-1,3,3a,4,9,9a-hexahydronaphtho[2,3-c]furan-6-ol (**8**) [12], α-conidendrin (**9**) [13], (7'*R*)-hydroxymatairesanol (**10**) [14], pinoresinol (**11**) [15], epipinoresinol (**12**) [16], *p*-hydroxybenzaldehyde (**13**), 4-(3-furanyl)phenol (**14**), and cycloeucalenol (**15**) [17].

3 Study of hypoglycaemic activity of representative compounds

The zebrafish (*Danio rerio*) has similar glucose metabolism pathways and metabolites with those of humans, which made it an ideal model for studying the hypoglycaemic activity of drugs [18, 19]. In this study, a *Tg (Ins:htBid $^{TE-ON}$;LR)* pancreatic β cells ablation zebrafish model was used to induce hyperglycaemic symptoms [20]. In the transgenic zebrafish, the truncated human Bid protein (htBid) was derived by an insulin promoter and controlled under the tetracycline- and ecdysone-inducible system. After induction with doxycycline (Dox) and tebufenozide (Tbf), the proapoptotic tBid expression in β cells resulted in the apoptosis of β cells, which were labelled by the transgenic line *Tg (− 1.2ins:H2Bmcherry).* The zebrafish was then incubated with compounds **1–17** (5 µmol/L) for 24 h as biological activity testing.

The free glucose level was significantly increased after the β cells' ablation compared with the non-induced transgenic zebrafish, suggesting that the β cells' ablation caused hyperglycaemia in the zebrafish model. Compounds **3, 5, 7, 11, 14** reduced glucose levels in the hyperglycaemic zebrafish, and compounds **5, 11, 14** had the most significant effect ($p < 0.001$) (Fig. 3A). We then tested the ED_{50} values of the hypoglycaemic activities of **5, 11, 14**, which were 1.46 ± 0.38, 2.01 ± 0.45, 2.67 ± 0.35 µmol/L respectively (Fig. 3B).

Inhibitory of blood glucose elevation mainly includes two mechanisms in different tissues: promotion of glucose uptake in peripheral tissue and regeneration of pancreatic β cells. Two zebrafish modes were applied to reveal the hypoglycemic mechanism.

Double transgenic zebrafish *Tg (Ins:htBid$^{TE−ON}$; LR); Tg (Ins:H2Bmcherry)* was applied to monitor the number of β cells after the treatment of compounds. The *Tg (Ins:H2Bmcherry)* zebrafish pulls red fluorescent protein (mCherry) to be expressed in the β cells under the regulation of an insulin-specific promoter and is used to label the β cells. Therefore, zebrafish pancreatic β cells can be observed, statistically and imaged through fluorescence microscopy [19]. Compared with the β cells ablation group (tBid + Dox + Tbf + DMSO), the number of pancreatic β cells in the hyperglycaemic zebrafish model did not change after 24 h of treatment with compounds **5, 11, 14** (Fig. 3C). This suggests that the hypoglycaemic activity of **5, 11, 14** is independent of pancreatic β cell regeneration.

Then we use the 2-NBDG, a glucose fluorescence analogue, was added in the zebrafish culture medium for indication of glucose uptake [21]. Experimental results show that compounds **5, 11, 14** can significantly increase the uptake of 2-NBDG in hyperglycaemic zebrafish, with similar activity of the positive drug rosiglitazone (RGZ). This indicates that compounds **5, 11, 14** can enhance the blood glucose uptake ability of hyperglycaemic zebrafish, which is the mechanism they exert hypoglycaemic activity (Fig. 3D).

4 Experimental section

4.1 General experimental procedures

Optical rotations were measured on a JASCO P-200 polarimeter (Tokyo, Japan). The UV spectra were recorded in methanol using a Shimadzu UV-260
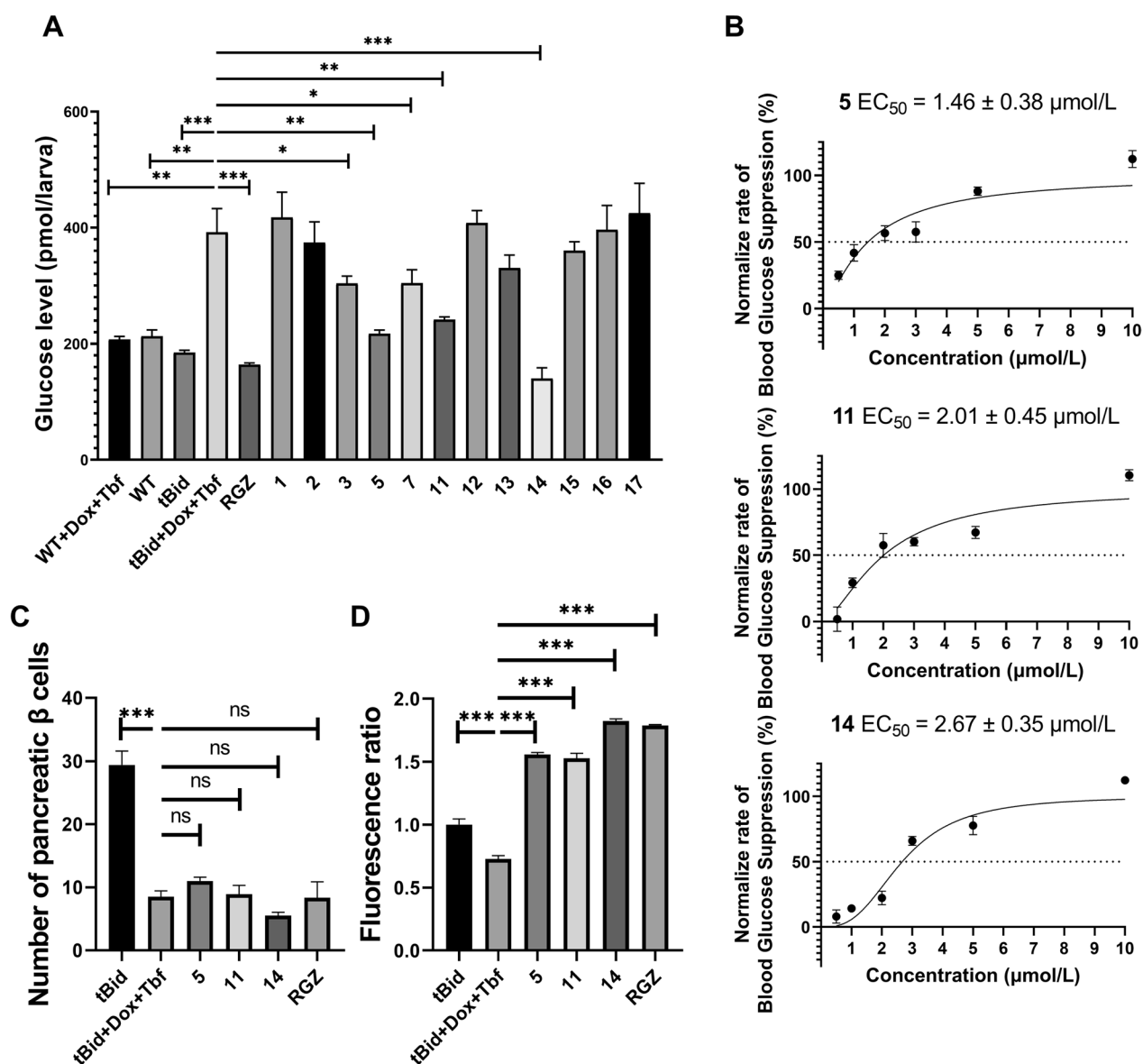
Yu et al. Natural Products and Bioprospecting   (2024) 14:23

Page 6 of 9

Fig. 3 Biological evaluation and mechanism study of the hypoglycaemic activity of isolated compounds. **A** Blood glucose value of hyperglycaemic zebrafish model after treatment with compounds **1–17** for 24 h. **B** ED_{50} value calculation of the hypoglycaemic activity of compounds **5**, **11**, **14**. **C** Changes in the number of pancreatic β cells in the hyperglycaemic zebrafish model after treatment with compounds **5**, **11**, **14** for 24 h. **D** Changes in the 2-NBDG uptake ability of the hyperglycaemic zebrafish model after treatment with compounds **5**, **11**, **14** for 24 h. (*$p < 0.05$; **$p < 0.01$; ***$p < 0.001$)

spectrophotometer (Kyoto, Japan). The ECD spectra were measured by a JASCO J-810 spectrometer (Tokyo, Japan). The IR measurements were performed on a Perkin-Elmer 683 spectrometer. The NMR experiments were conducted on Bruker Avance III-600 MHz spectrometers in CDCl$_3$ and DMSO-d_6. The HR ESIMS data were acquired using a Thermo Fisher Q-Exactive mass spectrometer (Boston, USA). Column chromatography (CC) separations were carried out by using silica gel (300–400 mesh; Qingdao Haiyang Chemical Co., Ltd., Qingdao, China), and ODS RP-C$_{18}$ (40–63 μm, FuJi, Aichi, Japan). An Agilent 1260 series system (California, USA) with an COSMOSIL 5C$_{18}$-MS-II (5 μm, 4.6 mm i.d. × 150 mm, Kyoto, Japan) column was used for HPLC analysis. Preparative HPLC was carried out using a Welch Sail 1000 series instrument equipped with a Welch Ultimate XB-C18 column (5 μm, 250 mm × 21.2 mm i.d., China).

Yu et al. Natural Products and Bioprospecting   (2024) 14:23

Page 7 of 9

4.2 Plant material

Dried wood of *Agathis dammara* (Lamb.) Rich was obtain from Xiamen Garden Botanical Garden (24° 26′ 54.6″ N 118° 06′ 26.4″ E) in March 2021, Xiamen, Fujian Province, China. A voucher specimen (2021BKS) was preserved in School of Pharmaceutical Sciences, Xiamen University, and identified by Associate Professor Quan-Cheng Chen.

5 Extraction and isolation

A total of 1 kg of dried *A. dammara* wood was extracted and refluxed for 3 times with 2 L of 95% ethanol for 1.5 h to concentrate to obtain 367 g of extract, which was suspended in water and then extracted with the same volume of dichloromethane to obtain 100 g of dichloromethane extract (Fr. A), first separated by silica gel column (petroleum ether-ethyl acetate 100:1–0:1), divided into 7 components (Fr. A1-Fr. A7).

After HPLC–DAD and TLC analysis, the scheme for further separation of Fr. A2-Fr. A6 was determined, that is, off-line separation by combining reversed-phase and normal-phase open chromatographic columns, combined with preparative HPLC. Each component was firstly passed through Chromatorex C_{18} as the chromatographic stationary phase, and carried out gradient elution using the conditions explored by HPLC analysis (MeOH–Water 5–100%). The eluted components were analyzed by TLC, using dichloromethane and methanol as developing solvents, and using a developing solvent formula with an Rf value of 0.2–0.3 on TLC as the mobile phase for silica gel column chromatography separation. The purity of the components separated at this time was checked by TLC and HPLC, and if impure, they were further purified by preparative HPLC (Additional file 1: Fig. S1).

5.1 Spectra data of the new compounds

(3β)-3,13-dihydroxykaur-16-en-2-one (**16**) is white powder, [α]20 D = 54°, melting point is 78.6 ~ 79.0 ℃. HR ESIMS shows that the molecular formula is $C_{20}H_{30}O_3$ (*m/z* 319.2265 [M+H]$^+$, calcd 319.2268), and the degree of unsaturation is 6. UV spectra indicated carbon–carbon double bond (λ_{max} = 210 nm), IR spectra indicated carbonyl (σ_{min} = 1712 cm^{-1}) and hydroxyl (σ_{min} = 3424 cm^{-1}).

2,13-dihydroxykaura-1,16-dien-3-one (**17**) is white powder, [α]20 D = 24°, melting point is 118.8 ~ 121.2 ℃. HR ESIMS showed that the molecular formula is $C_{20}H_{28}O_3$ (*m/z* 317.2108 [M+H]$^+$, calcd 317.2111), and the degree of unsaturation is 7. UV spectra indicated carbon–carbon double bond (λ_{max} = 210 nm) and α, β-unsaturated ketone (λ_{max} = 270 nm), IR

spectra indicated carbonyl (σ_{min} = 1711 cm^{-1}), hydroxyl (σ_{min} = 3425 cm^{-1}) structure. Their NMR data are listed in Table 1.

5.2 ECD calculations

Conformational analyses were performed by Schrodinger Maestro 12.8 using Conformational Search function. The output conformers were then optimized at OPLS4 force field and filtered by RMSD threshold of 0.1 Å and energy window of 5.02 kcal/mol. The conformations calculated according to the Boltzmann equation at room temperature accounted for less than 1% were removed, and the five conformations with the energy closest to the lowest energy conformation were screened to calculate the excitation spectrum. The theoretical calculations were carried out using Gaussian 09W. The chosen conformers were finally optimized at B3LYP/6-31G(d) in methanol.

The ECD calculations of the chosen conformers were executed in methanol with Time-dependent Density functional theory (TD-DFT) at B3LYP/6−31+G(d) or B3LYP/6−311+G(d,p) level by Gaussian 09W. Rotatory strengths for 20 or 30 excited states were calculated. Finally, GaussView 6.0 was used to add the spectrum according to the energy of various conformations according to the Boltzmann energy equation to obtain the ECD calculation spectrum.

5.3 Establishment and treatment of hyperglycemic zebrafish model

Fertilized eggs of zebrafish strain *Tg (Ins:htBid$^{TE−ON}$, Ins:H2Bmcherry)* were collected the next day, and this time was recorded as day 0 post fertilization (0 dpf). Tbf (3 μL, 50 mmol/L) and Dox (3 μL, 100 mmol/L) were added into a 3.5 cm cell culture dish containing 6 mL 0.3 × Danieau's buffer. Then, the dish was placed in a zebrafish incubator without light for 48 h to induce β cells in 2 dpf ablation.

Diabetic zebrafish that were ready to be used in experiments after β cells ablation were rinsed with 0.3 × Danieau's buffer to remove Tbf and Dox. The larvae were placed into a 24-well plate at a density of 10 zebrafishes/well, in 2 mL of egg water. All compounds were made in 10 mM with DMSO (prepare other concentrations when calculating ED$_{50}$). For the treatment, each group was added accordingly with 2 mL of egg water treated with 1 μL of each of the compounds (10 mmol/L) to reach the final concentration of (5 μmol/L), and the control group was treated with the same amount of DMSO. The treatments lasted for 24 h in the zebrafish incubator. The group of tBid which was not induced with Tbf and Dox was used as a control of normal zebrafish.

Yu *et al. Natural Products and Bioprospecting*   (2024) 14:23

Page 8 of 9

Table 1 ^{13}C-NMR (150 MHz, CDCl$_3$) and ^{1}H-NMR (600 MHz, CDCl$_3$) spectrum data of compounds **16** and **17**

No.	16		17		Excoecarin K
	δ_H (mult., *J* in Hz)	δ_C	δ_H (mult., *J* in Hz)	δ_C	δ_C
1	2.03 m; 2.64, dd (12.90, 2.00)	53.2	6.45 m	128.4	53.4
2		210.7		144.3	211.0
3	3.87, br s	82.8		201.0	82.8
4		45.3		44.0	45.3
5	1.49, m	54.4	1.68 m	53.9	55.4
6	1.45, m; 1.72, m	20.1	1.55 m; 1.58 m	20.4	20.1
7	1.61, 1.60 m	40.6	1.62 m; 1.65 m	40.6	39.2
8		41.7		41.8	45.5
9	1.29, br s	54.0	1.28 s	49.4	55.4
10		45.2		40.0	44.3
11	1.66, m; 1.67, m	20.4	1.92 m; 1.77 m	20.6	18.4
12	1.58, m; 1.80, m	39.0	1.61 m; 1.82 m	39.0	32.8
13		80.0		80.0	43.7
14	1.28, m; 2.04, m	46.4	2.11 dd (11.0, 2.7);1.33 dd (11.0, 2.7)	47.4	40.5
15	2.12, br d (17.1); 2.27, dd (17.1, 2.0)	47.1	2.11 m;2.27 m	47.3	48.7
16		155.3		155.3	154.9
17	4.85, m; 5.00, m	103.5	4.87 s; 5.03 t (2.6)	103.7	103.6
18	0.70, br s	16.6	1.14 s	21.5	18.6
19	1.19, s	29.7	1.21 s	27.7	29.7
20	0.97, s	18.6	1.30 s	22.0	16.4

5.4 Total glucose level test

After the compound treatment, a pool of 10 larvae was homogenized in 100 μL of sample buffer. The homogenate was spun at 10,000 rpm for 10 min. Free glucose in 10 μL of supernatant (equivalent of one larva) was determined according to the manufacturer's instructions. Fluorescence (excitation, 520 nm; emission, 580–640 nm) was measured using a SpectraMax M5 Microplate Reader (Molecular Devices, California, USA). Each sample was measured for three pools. The obtained data were imported into GraphPad Prism 8.0.2 software, and the statistical differences among the groups were analyzed using the t-test method.

5.5 2-NBDG test

After the compound treatment, zebrafish (6 dpf) were incubated in a culture medium containing 600 μmol/L 2-NBDG (Apexbio, B6035, Texas, USA) for 3 h. A pool of 5 larvae was homogenized in 100 μL of sample buffer. The homogenate was spun at 10,000 rpm for 10 min. The supernatant (30 μL) was placed into a 96-well plate to detect fluorescence (excitation, blue 475 nm; emission, 500–550 nm) using a SpectraMax M5 Microplate Reader (Molecular Devices, California, USA). Each sample was measured for three pools. The obtained data were imported into GraphPad Prism 8.0.2 software, and the

statistical differences among the groups were analyzed using the ordinary one-way (ANOVA) method.

5.6 Microscopic imaging and counting of pancreatic cells

The compounds with 0.3 × Danieau's buffer were washed out after the compound treatment in 24 h. The larvae with 4% paraformaldehyde were fixed overnight at 4 °C and placed on a slide with aqua-mount (Richard-AllanScientific, Michigan, USA) with the right sides of the larvae facing up to expose the islets. The number of cells number was counted according to the RFP and GFP under a Leica TCS SP8 microscope (Leica, Weztlar, Germany) with 63 × lens. Microscopic images were processed and counted by LASX Office 1.4.5 software. The obtained data were imported into GraphPad Prism 8.0.2 software, and the statistical differences among the groups were analyzed using the ordinary one-way (ANOVA) method.

6 Conclusion

In summary, two new kaurane diterpenes (3β)-3,13-dihydroxykaur-16-en-2-one (**16**) and 2,13-dihydroxykaura-1,16-dien-3-one (**17**) along with 15 known compounds were isolated from the woods of *A. dammara*. Among them, three compounds **5**, **11**, and **14** showed significant hypoglycaemic activity in the hyperglycaemic zebrafish model. Further mechanism analysis

Yu *et al. Natural Products and Bioprospecting*   (2024) 14:23

Page 9 of 9

showed that this activity was caused by improving the glucose uptake ability of zebrafish. These findings enrich the structural diversity of diterpenes from the genus *Agathis* and provide potential lead compounds for the development of naturally derived antihyperglycemic drugs.

Supplementary Information

The online version contains supplementary material available at https://doi.org/10.1007/s13659-024-00440-4.

Additional file 1: Spectral data, mass data and calculation details of new compounds, and flow diagram of compounds separation.

Author contribution
Zhe-Wei Yu organized and wrote the manuscript. Bang-Ping Cai was responsible for the identification of plant. Yi Zhang, Wen-Hui Wang and Qi Chen were responsible for completing zebrafish activity experiments. Shun-Zhi Liu and Yan-Lin Bin completed some of the separation work. Mei-Juan Fang elucidated the spectrum data. Rong Qi is responsible for the manuscript revision. Su-Zhi Xie, Ming-Yu Lin and Ying-Kun Qiu proposed the study topic ideas. The authors read and approved the final manuscript.

Availability of data and materials
The datasets used or analysed during the current study are available from the corresponding author on reasonable request.

Declarations

Ethics approval and consent to participate
All procedures have been approved by the Xiamen University Institutional Animal Care and Use Committee (Protocol XMULAC20160089, 10 March 2016). Informed consent was obtained from all individual participants included in the study.

Competing interests
The authors declare no conflict of interest.

Author details
[1]School of Pharmaceutical Sciences, Xiamen University, Xiamen 361102, China. [2]School of Basic Medical Sciences, Peking University, Beijing 100191, China. [3]Xiamen Botanical Garden, Xiamen 361003, Fujian, China. [4]Xiamen Medical College Affiliated Haicang Hospital, Xiamen 361026, China.

References
1. Zhang X. Research on the introduction and cultivation of *Agathis dammara* and seedling breeding technology. Straits Sci. 2002;05:41–2+44.
2. Wang A, Yue S, Peng A, Qi R. A review of research progress on *Agathis dammara* and its application prospects for cardiovascular diseases and fatty liver disease. Mini-Rev Med Chem. 2021;21(6):670–6.
3. Xiao D. Damar Minyak of Agathis. Furnit Interior Des. 2013;12:90–3.
4. Zhang Q, Cai Z, Yu Z, Di C, Qiu Y, Qi R. *Agathis dammara* extract and its monomer Araucarone attenuate abdominal aortic aneurysm in mice. Cardiovasc Drugs Therapy. 2023. https://doi.org/10.1007/s10557-023-07518-0.
5. Konishi T, Konoshima T, Fujiwara Y, Kiyosawa S. Excoecarins D, E, and K, from *Excoecaria agallocha*. J Nat Prod. 2000;63(3):344–6.
6. Takaku N, Choi D, Mikame K, Okunishi T, Suzuki S, Ohashi H, Umezawa T, Shimada M. Lignans of *Chamaecyparis obtusa*. J Wood Sci. 2001;47(6):476–82.
7. Li X, Cai J, Wang W, Ai H, Mao Z. Two new acetylenic compounds from *Asparagus officinalis*. J Asian Nat Prod Res. 2016;18(4):344–8.
8. Zhang Y, Tan N, Yang Y, Lu Y, Cao P, Wu Y. Norlignans from *Sequoia sempervirens*. Chem Biodivers. 2005;2(4):497–505.
9. Tang J, Fan G, Dai F, Ding D, Wang Q, Lu D, Li R, Li X, Hu L, Jin X, Zhou B. Finding more active antioxidants and cancer chemoprevention agents by elongating the conjugated links of resveratrol. Free Radic Biol Med. 2011;50(10):1447–57.
10. Leyi H, Yuzheng S, Qianqian C, Tingting D, Hongtao X, Guixin C. Chemical constituents of *Patrinia villosa*. Chin Tradit Herb Drugs. 2021;52(23):7088–95.
11. Li H, Li X, Wang J. Chemical constituents of Nux Prinsepiae Uniflorae. J Shenyang Pharm Univ. 2006;04:209–11.
12. Cambie RC, Clark GR, Craw PA, Jones TC, Rutledge PS, Woodgate PD. Chemistry of the Podocarpaceae. LXIX. Further lignans from te wood of Dacrydium intermedium. Aust J Chem. 1985;38(11):1631–45.
13. Zhou X, Yu F, Zeng Q. Study on the chemical composition of *Taxus yunnanensis* heartwood. Tradit Chin Drug Res Clin Pharmacol. 2002;05:317–9.
14. Jingi W, Yanzi M, Chunxue Z, Qinxue J, Huming H, Jiao B. Lignans from stems and leaves of *Cephalotaxus fortunei*. Chin Tradit Herb Drugs. 2020;51(01):36–42.
15. Chang CI, Hsu CM, Li TS, Huang SD, Lin CC, Yen CH, Chou CH, Cheng HL. Constituents of the stem of *Cucurbita moschata* exhibit antidiabetic activities through multiple mechanisms. J Funct Foods. 2014;10:260–73.
16. Okuyama E, Suzumura K, Yamazaki M. Pharmacologically active components of Todopon Puok (Fagraea racemosa), a medicinal plant from Borneo. Chem Pharm Bull. 1995;43(12):2200–4.
17. Yang Y, Liu J. The constituents of Ervatamia divaricata. Acta Botanica Yunnanica. 1999;21(2):260–4.
18. Heckler K, Kroll J. Zebrafish as a model for the study of microvascular complications of diabetes and their mechanisms. Int J Mol Sci. 2017;18(9):2002.
19. Jia JX, Kang Q, Liu SZ, Song YB, Wong FS, Qiu YK, Li MY. Artemether and aspterric acid induce pancreatic alpha cells to transdifferentiate into beta cells in zebrafish. Br J Pharmacol. 2022;179(9):1962–77.
20. Li M, Maddison LA, Page-McCaw P, Chen W. Overnutrition induces β-cell differentiation through prolonged activation of β-cells in zebrafish larvae. Am J Physiol Endocrinol Metab. 2014;306(7):E799-807.
21. Lee J, Jung D, Kim W, Um J, Yim S, Oh WK, Williams DR. Development of a highly visual, simple, and rapid test for the discovery of novel insulin mimetics in living vertebrates. ACS Chem Biol. 2013;8(8):1803–14.